




Phosphorus spectroscopy in acute TBI demonstrates metabolic changes that relate to outcome in the presence of normal structural MRI

Matthew G Stovell¹ , Marius O Mada², T Adrian Carpenter², Jiun-Lin Yan^{1,3}, Mathew R Guilfoyle¹, Ibrahim Jalloh¹, Karen E Welsh², Adel Helmy¹, Duncan J Howe⁴, Peter Grice⁴, Andrew Mason⁴, Susan Giorgi-Coll¹, Clare N Gallagher^{1,5}, Michael P Murphy⁶, David K Menon^{2,7}, Peter J Hutchinson^{1,2,*} and Keri LH Carpenter^{1,2,*}

Abstract

Metabolic dysfunction is a key pathophysiological process in the acute phase of traumatic brain injury (TBI). Although changes in brain glucose metabolism and extracellular lactate/pyruvate ratio are well known, it was hitherto unknown whether these translate to downstream changes in ATP metabolism and intracellular pH. We have performed the first clinical voxel-based *in vivo* phosphorus magnetic resonance spectroscopy (³¹P MRS) in 13 acute-phase major TBI patients versus 10 healthy controls (HCs), at 3T, focusing on eight central 2.5 × 2.5 × 2.5 cm³ voxels per subject. PCr/γATP ratio (a measure of energy status) in TBI patients was significantly higher (median = 1.09) than that of HCs (median = 0.93) ($p < 0.0001$), due to changes in both PCr and ATP. There was no significant difference in PCr/γATP between TBI patients with favourable and unfavourable outcome. Cerebral intracellular pH of TBI patients was significantly higher (median = 7.04) than that of HCs (median = 7.00) ($p = 0.04$). Alkalosis was limited to patients with unfavourable outcome (median = 7.07) ($p < 0.0001$). These changes persisted after excluding voxels with > 5% radiologically visible injury. This is the first clinical demonstration of brain alkalosis and elevated PCr/γATP ratio acutely after major TBI. ³¹P MRS has potential for non-invasively assessing brain injury in the absence of structural injury, predicting outcome and monitoring therapy response.

Keywords

³¹P magnetic resonance spectroscopy, adenosine triphosphate, clinical outcome, pH, traumatic brain injury (human)

Received 12 March 2018; Revised 5 August 2018; Accepted 3 August 2018

Introduction

Traumatic brain injury (TBI) is a major cause of death and disability worldwide, placing high demands on carers and resources.¹ Neurosurgical and neurocritical care attempt to support the brain's recovery through a

⁴Department of Chemistry, University of Cambridge, Cambridge, UK

⁵Division of Neurosurgery, Department of Clinical Neurosciences, University of Calgary, Calgary, Alberta, Canada

⁶MRC Mitochondrial Biology Unit, University of Cambridge, Cambridge, UK

⁷Division of Anaesthesia, Department of Medicine, University of Cambridge, Cambridge, UK

*Joint senior authors.

Corresponding authors:

Matthew G. Stovell and Keri L.H. Carpenter, Division of Neurosurgery, Department of Clinical Neurosciences, University of Cambridge, Box 167, Cambridge Biomedical Campus, Cambridge, CB2 0QQ, UK. Email: mgs48@cam.ac.uk and klc1000@wbc.cam.ac.uk

¹Division of Neurosurgery, Department of Clinical Neurosciences, University of Cambridge, Cambridge, UK

²Wolfson Brain Imaging Centre, Department of Clinical Neurosciences, University of Cambridge, Cambridge, UK

³Department of Neurosurgery, Keelung Chang Gung Memorial Hospital, Chang Gung University College of Medicine, Taoyuan, Taiwan

critical period when the damaging pathophysiological processes of secondary brain injury occur. A key contributor to secondary brain injury is cerebral metabolic dysfunction. Acute TBI patients often show elevated concentration of extracellular lactate relative to pyruvate (high L/P ratio) despite showing seemingly adequate cerebral perfusion pressure and local brain tissue oxygen.^{2,3} This is attributed to a failure of mitochondrial function^{4,5} as L/P ratio represents reduced/oxidised nicotinamide adenine dinucleotide (NADH/NAD⁺) redox state.⁶

It is unclear whether this translates to a change in high-energy phosphates in the acute phase after severe TBI. ATP is principally produced by mitochondrial oxidative phosphorylation and is also synthesised in the cytosol via glycolysis. The brain also contains the high-energy phosphate species phosphocreatine (PCr), which is most abundant in tissues requiring energy in bursts, e.g. muscle and brain. PCr acts as a reserve that can be rapidly mobilised for fast recycling of ADP to ATP to drive cellular processes in times of high demand, thereby acting as a temporal buffer for ATP; and due to its greater free diffusion in the cytoplasm compared to ATP and ADP, it also serves as a spatial buffer, smoothing out spatial variations in cellular energy state.^{7,8} A high brain extracellular L/P ratio acutely after severe TBI implies diversion of pyruvate away from entry into the tricarboxylic acid (TCA) cycle to maintain flux through glycolysis, which is likely to limit oxidative phosphorylation. However, changes in brain energy storage, expressed as PCr/ATP ratio, have not previously been investigated within the human brain during the acute phase of injury.

Here, we demonstrate the first voxel-based in vivo phosphorus magnetic resonance spectroscopy (³¹P MRS) study of brain energetics in severe acute TBI in humans. Steady-state in vivo ³¹P MRS is a non-invasive technique for interrogating high-energy phosphate species, including ATP and PCr, inorganic phosphate (Pi) and brain pH, by using a dedicated ³¹P head coil (Figure 1) – using relative concentrations of these metabolites (rather than rates of flux) to report the state of brain energy metabolism. This is the first voxel-based in vivo chemical shift imaging ³¹P MRS study of brain energetics and pH in humans in the acute phase of moderate-severe TBI.¹ Our state-of-the-art clinical MR scanning has yielded high-quality well-resolved ³¹P spectra with a good baseline, enabling reliable measurement of metabolites in multiple voxels per patient. 3D localisation has allowed accurate assessment of grey/white matter ratio and radiological injury of each voxel. Our scanner's location directly adjacent to the neurosciences critical care unit has enabled us to focus on severe TBI patients in the acute phase, whilst fully sedated and ventilated.

We report changes in brain energy metabolism and intracellular pH in the acute phase of major TBI, evaluate how these data relate statistically to patients' clinical outcomes after six months and identify altered brain metabolism in brain that appears uninjured on MRI sequences sensitive to pathology.

Materials and methods

Study design, patients and healthy controls

We recruited patients (aged over 16 years) who had sustained moderate or severe TBI (defined as cranial trauma with consistent CT scan findings and a post-resuscitation Glasgow Coma Scale (GCS) ≤ 12) that required sedation and mechanical ventilation for intracranial hypertension and airway protection (Table 1) – which we describe as 'major' TBI. Two patients who presented initially with moderate TBI (GCS 10) deteriorated during resuscitation to GCS ≤ 8 . Patients were treated using our standard TBI management protocols including: endotracheal intubation, ventilation, sedation, muscular paralysis and maintenance of blood sugar (serum glucose) concentration within the target range 4–10 mmol/L.⁹ Scans were in the acute phase as soon as patients' intracranial pressure permitted them to be laid supine, whilst still requiring full sedation, ventilation and monitoring for control of intracranial hypertension. Of our 13 patients, 9 were scanned within a week of primary injury and 4 within two weeks of injury because their persistent brittle intracranial hypertension precluded them from being laid supine for MR any sooner. Arterial blood samples were taken and analysed for pH and partial pressure of CO₂ (PaCO₂) before and after patients' scans, and the average of the two results was calculated. Informed written assent was obtained from the patients' relatives, and age-group-matched healthy controls were recruited locally with their informed written consent. The study conformed to the spirit and the letter of the Declaration of Helsinki. Protocol approval was by the National Research Ethics Service (NRES) Committee East of England – Cambridge Central (REC Reference No. 11/EE/0463). Patients' six-month follow-up included Glasgow Outcome Scale Extended¹⁰ (GOS-E) scoring, assessed without knowledge of study results. Outcome was dichotomised into upper severe disability or better (GOS-E ≥ 4 ; independent at home) and lower severe disability or worse (GOS-E ≤ 3 ; dependent at home, vegetative or dead), as in other recent studies.^{11,12}

Magnetic resonance spectroscopy

We used 3 Tesla Siemens (Trio and Verio) scanners with a custom ³¹P head-coil (PulseTeq Ltd,

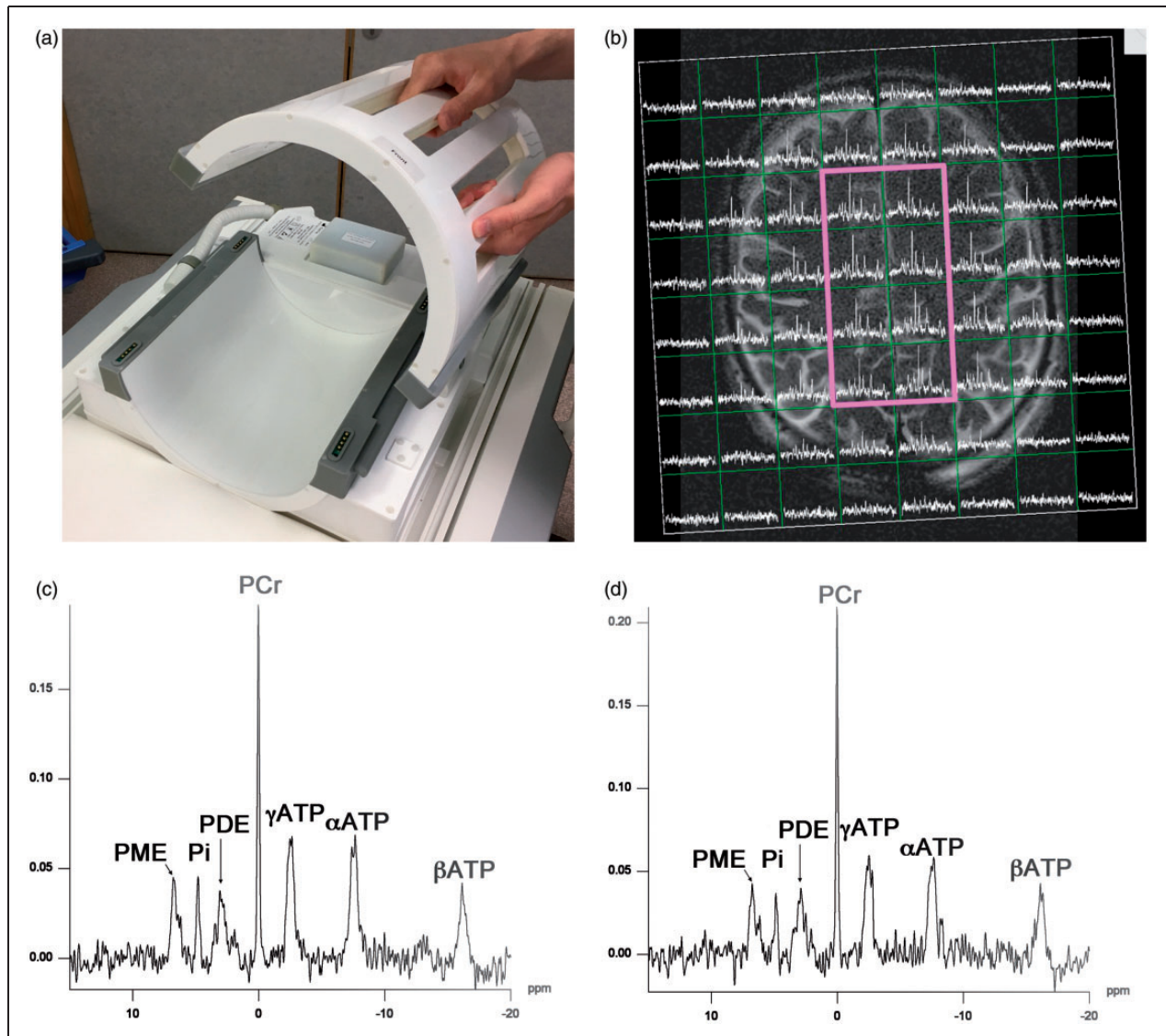


Figure 1. ^{31}P MRS acquisition. (a): Custom-built (PulseTeq Ltd) birdcage ^{31}P head-coil for use on Siemens 3-Tesla magnetic resonance (MR) imaging scanner. The head-coil opens to facilitate use with patients. Image is courtesy of the Wolfson Brain Imaging Centre. (b): Example of axial T2 weighted MRI scan (Siemens 3 T) with ^{31}P MR spectra overlaid in a grid of voxels using the custom head-coil (Pulseteq Ltd) in a healthy control. The eight central voxels within the bold magenta outline were used for data analysis. (c and d): Example ^{31}P spectrum from a central voxel in a healthy control (c) and traumatic brain injury patient (d), with 200 ms Hanning filter. Metabolite peaks labelled. PE: phosphomonoesters; Pi: inorganic phosphate; PDE: phosphodiester; PCr: phosphocreatine; ATP: adenosine triphosphate.

Chobham, UK) (Figure 1(a)) with a birdcage design that opens to facilitate use with our patients, measuring ATP, PCr, Pi and other phosphorus-containing species. Spectra were acquired using oblique two-dimensional single slice chemical shift imaging (2D CSI) with $2.5 \times 2.5 \times 2.5 \text{ cm}^3$ voxels, flip angle 90 degrees, TR 4000 ms, TE 2.3 ms and 3000 Hz bandwidth. Repeats were performed for 30 (19 min) or 60 (35 min) averages. Weighted sampling of k-space was performed. Patients also received ^1H clinical MR imaging, including sequences sensitive for detecting injury: fluid-attenuated

inversion recovery (FLAIR) and susceptibility weighted imaging (SWI). ^{31}P spectra were filtered with a 200 ms Hanning filter, fitted and peak areas computed using Siemens Syngo software. Absolute concentrations are difficult to accurately quantify with in vivo clinical ^{31}P MRS, so we used the ratio of PCr to γATP signal intensities of the fitted spectra as our primary measure of high-energy phosphate metabolic status.^{13,14} We employed γATP , the ‘cleanest’ of the three ATP signals. We did not use the βATP peak as it is not reliably excited due to being at the edge of our excitation

Table 1. Demography of traumatic brain injury patients.

Subject number	Age group	Sex	Injury mechanism	Brain injury	GCS total	GCS E, V, M	Days from TBI	GOS-E six months	Outcome
P01	20–34	M	Assault	EDH, brain contusions	8	E1V2M5	5	3	Unfav.
P02	50–65	F	Fall from height	ASDH, ICH	7	E2V1M4	3	5	Fav.
P03	35–49	M	Assault	DAI, hypoxia	8	E3V4M1	10	2	Unfav.
P04	50–65	M	RTC	EDH, ICH	3	E1V1M1	4	1	Unfav.
P05	50–65	M	Presumed assault	ASDH, brain contusions	10	E4V2M6	7	2	Unfav.
P06	20–34	M	RTC	brain contusions	6	E1V1M4	4	5	Fav.
P07	35–49	M	Fall from height	ASDH, brain contusions	8	E2V1M5	5	5	Fav.
P08	35–49	M	RTC	ASDH	6	E1V1M4	11	5	Fav.
P09	35–49	M	Assault	ASDH, EDH, brain contusions	6	E1V2M3	4	1	Unfav.
P10	50–65	F	RTC	EDH, brain contusions	10	E3V1M6	6	1	Unfav.
P11	20–34	F	RTC	brain contusions	5	E1V2M2	14	4	Fav.
P12	20–34	M	RTC	brain contusions	7	E1V1M5	13	5	Fav.
P13	50–65	M	Assault	ASDH, brain contusions	4	E1V1M2	4	5	Fav.

Note: Age group in years. GCS denotes highest GCS at presentation to emergency services. Patients P5 and P10 presented as only moderately drowsy, but then rapidly deteriorated, requiring sedation, intubation, ventilation and surgery for their TBI followed by a period of intracranial multimodality monitoring and treatment for intracranial hypertension. Patients P03, P08, P11 and P12 had persistently high ICP that was difficult to control and were scanned as soon as they could tolerate lying flat. At the time of the scans, they still required sedation, ventilation and active ICP control, thus still representing the ‘acute phase’ after TBI.

M: male, F: female, RTC: road traffic collision, GCS: Glasgow Coma Scale score, E: eye response, V: verbal response, M: motor response, L: left, R: right, EDH: extradural haematoma, ASDH: acute subdural haematoma, ICH: intracerebral haematoma, GOS-E: Glasgow outcome score (Extended), Outcome: favourable (Fav.) GOS-E ≥ 4 ; unfavourable (Unfav.) GOS-E ≤ 3 .

bandwidth at 3T, and we did not use the α ATP peak as it is incompletely resolved from NAD and NADH. We did not attempt to adjust ATP values for the presence of ADP as it is naturally much less abundant, e.g. ATP ≈ 3 mmol/L, ADP < 100 μ mol/L¹⁵ and mostly MR-invisible.^{16,17} To indicate whether variation in PCr/ γ ATP ratio was driven principally by changes in PCr or γ ATP, we assessed the ratio of PCr to total-mobile-phosphate (defined as the combined signals PCr plus γ ATP plus Pi) and the ratio of γ ATP to total-mobile-phosphate.^{13,14} The PCr, γ ATP and Pi resonances together represent the total mobile high-energy phosphate pool involved directly with ATP metabolism. Intracellular pH was calculated from the chemical shift difference between PCr and Pi, using an established equation.^{18,19}

Voxel tissue type (grey matter, white matter and CSF) was segmented using FAST (FMRIB’s Automated Segmentation Tool) processing of 3D T1W gradient echo sequences (MP RAGE) in FSL (FMRIB software, Oxford, UK). Regions of FLAIR and SWI radiological injury were reviewed and manually mapped. Ratios of grey matter/white matter and radiologically visible injury were then calculated for each voxel using Matlab software (MathWorks, Natick, MA). Our primary inclusion criterion for data analysis was that voxels contained at least 90% brain tissue; voxels with less than 90% brain tissue were excluded at the outset. A sub-analysis of ‘radiologically-normal’ brain was performed

by further excluding voxels with more than 5% injury on FLAIR or SWI. As part of a separate biochemical study, nine voxels were supplemented (via a microdialysis catheter, prior to scan) with succinate or glucose, and therefore were excluded from the present data analysis.²⁰

Statistical analysis

Statistical analysis was performed in R (www.r-project.org). Comparison of PCr/ γ ATP, PCr/total-mobile-phosphate, γ ATP/total-mobile-phosphate and pH between healthy controls and TBI patients was performed with subject-mean data, using Mann-Whitney U test, and repeated using a linear mixed effects model (‘lme’ in R package nlme²¹) of pooled data, which accounts for ‘clustering’ of data as each subject contributes multiple voxels. Further comparisons of high-energy phosphate ratios and pH between TBI patients with ‘favourable outcome’ (GOS-E ≥ 4) and ‘unfavourable outcome’ (GOS-E ≤ 3) were also performed with Mann-Whitney U of subject-mean data and lme of individual voxels, using generalised linear hypothesis tests (glht) with Bonferroni correction when healthy controls were included in the model of patient outcome. Voxel grey matter/white matter ratio was included as a covariate in all mixed effect models. The relationship between brain pH and PCr/ATP ratio, arterial blood pH and PaCO₂ was assessed with Spearman’s rank

correlation. Potential confounders/nuisance variables were explored using Spearman's rank correlation and Mann-Whitney U tests. Results quoted for outcome are group medians of within-patient means. Graphs were plotted with R and Origin.

Data availability

This study's datasets are not publicly available because of patient confidentiality, but anonymised data are available from Prof Peter Hutchinson (the Principal Investigator), on reasonable request.

Results

In vivo ^{31}P MRS data were available for a total of 90 voxels from 13 sedated, ventilated TBI patients (nine male, four female), median age 42 years, range 24–65 years, and 80 voxels from 10 age-group and sex-matched healthy control subjects. Patients' demography is given in Table 1, and healthy controls are given in Supplementary Table 1. No clinical complications resulted from MRS. An example scan is shown in Figure 1(b) and ^{31}P spectra examples are shown in Figure 1(c) and (d). Summary ^{31}P MRS data are given in Table 2 and individual patient data are given in Table 3. Our scans were performed as early after injury as clinically feasible, whilst patients still required deep sedation and neurocritical

care, so were regarded as within the 'acute phase' of injury.

^{31}P MRS: metabolic changes in acute TBI

We first compared the high-energy phosphate ratios and pH of TBI patients and age-group matched healthy controls with Mann-Whitney U test, using each subject's mean value calculated from the central eight voxels of their brains. PCr/ γ ATP was higher in TBI patients (Figure 2(a)): median (and interquartile range, IQR) PCr/ γ ATP was 1.09 (1.04–1.20) in TBI patients and 0.93 (0.86–0.96) in healthy controls ($p < 0.0001$). PCr/total-mobile-phosphate was also higher in TBI patients (Figure 2(c)): median PCr/total-mobile-phosphate was 0.47 (0.46–0.48) in TBI patients and 0.42 (0.41–0.43) in healthy controls ($p < 0.0001$); whereas γ ATP/total-mobile-phosphate was lower in TBI patients (Figure 2(d)): median γ ATP/total-mobile-phosphate was 0.44 (0.40–0.45) in TBI patients and 0.46 (0.45–0.48) in healthy controls ($p = 0.0003$). TBI patients' brain pH was more alkaline than that of healthy controls (Figure 2(b)): median 7.04 (7.02–7.05) in TBI patients; and 7.00 (6.99–7.00) in healthy controls ($p = 0.006$). Intracellular pH correlated significantly with PCr/ γ ATP (Figure 3(a)). This association was not strong (Spearman's correlation coefficient $\rho = 0.27$), although highly statistically significant ($p < 0.0001$). There was a statistically significant inverse

Table 2. Summary of ^{31}P MRS results: group medians and interquartile ranges of within-subject means.

	Number subjects	Injured voxels	PCr/ γ ATP Median (IQR)	PCr/total Median (IQR)	γ ATP/total Median (IQR)	pH Median (IQR)
TBI: all patients	13	Including	1.09 (1.04–1.20)	0.47 (0.46–0.48)	0.44 (0.40–0.45)	7.04 (7.02–7.05)
		Excluding	1.07 (1.06–1.21)	0.47 (0.46–0.49)	0.44 (0.40–0.45)	7.03 (7.01–7.05)
Healthy controls	10	NA	0.93 (0.86–0.96)	0.42 (0.41–0.43)	0.46 (0.45–0.48)	7.00 (6.99–7.00)
p (TBI vs. HC)		Including	<0.0001	<0.0001	0.0009	0.042
		Excluding	<0.0001	<0.0001	0.001	0.055
TBI: favourable outcome	7	Including	1.07 (1.04–1.10)	0.48 (0.46–0.48)	0.44 (0.44–0.45)	7.02 (7.00–7.03)
		Excluding	1.07 (1.06–1.09)	0.47 (0.46–0.48)	0.44 (0.44–0.45)	7.02 (7.00–7.03)
TBI: unfavourable outcome	6	Including	1.14 (1.07–1.22)	0.47 (0.46–0.49)	0.41 (0.39–0.42)	7.07 (7.04–7.14)
		Excluding	1.14 (1.06–1.24)	0.48 (0.47–0.49)	0.41 (0.40–0.44)	7.07 (7.03–7.16)
p (Fav vs. Unfav.)		Including	0.3	0.9	0.04	0.03
		Excluding	0.3	0.9	0.06 [0.04]	0.057 [0.008]

Note: ^{31}P magnetic resonance spectroscopy (MRS) measurements of pH, phosphocreatine (PCr), adenosine triphosphate (γ ATP) and 'total' mobile phosphate (PCr + γ ATP + inorganic phosphorus) ratios in 13 patients suffering from acute major traumatic brain injury (TBI) and 10 age-group matched healthy controls (HC). Results represent group medians of within-subject means, with interquartile ranges (IQR) in parentheses (curved brackets); for each individual subject's mean values see Table 3. Voxels were considered injured if they contained $\geq 5\%$ radiological injury on fluid-attenuated inversion recovery (FLAIR) or susceptibility weighted injury (SWI) MR sequences. Favourable outcome (Fav) defined as six-month Glasgow outcome score (extended) (GOS-E) ≥ 4 , and unfavourable outcome (Unfav.) GOS-E ≤ 3 . Statistical analysis performed using a linear mixed model in R (lme in package nlme), adjusting for voxel grey matter/white ratio. Inclusion of healthy controls and analysis of the linear model using glht (results in Figure 4) found the difference in γ ATP/total-mobile-phosphate to be statistically significant (results in square [] brackets), but did not affect the significance of other measurements.

Table 3. ^{31}P MRS data acquired from TBI patients and healthy controls.

Subject ID	PCr/ γ ATP mean	PCr/ γ ATP S.D.	PCr/total mean	PCr/total S.D.	γ ATP/total mean	γ ATP/total S.D.	pH mean	pH S.D.	No. of voxels
P01	1.06	0.11	0.47	0.03	0.45	0.02	7.03	0.09	7
P02	1.10	0.17	0.48	0.04	0.44	0.03	7.02	0.03	7
P03	1.41	0.13	0.52	0.04	0.37	0.03	7.29	0.07	7
P04	1.00	0.12	0.42	0.06	0.42	0.04	7.15	0.09	7
P05	1.09	0.23	0.46	0.06	0.42	0.04	7.10	0.07	4
P06	1.07	0.14	0.48	0.04	0.45	0.02	7.01	0.07	6
P07	1.03	0.13	0.45	0.03	0.45	0.02	6.98	0.02	8
P08	1.21	0.13	0.48	0.04	0.40	0.04	7.02	0.06	8
P09	1.20	0.04	0.47	0.02	0.39	0.02	7.05	0.05	6
P10	1.23	0.09	0.49	0.03	0.40	0.03	7.04	0.02	7
P11	1.04	0.05	0.46	0.01	0.44	0.02	7.04	0.02	7
P12	1.04	0.08	0.46	0.03	0.44	0.01	7.04	0.07	8
P13	1.10	0.28	0.50	0.06	0.46	0.05	6.96	0.06	8
H01	0.95	0.07	0.42	0.02	0.45	0.01	6.99	0.02	8
H02	0.74	0.07	0.37	0.02	0.50	0.02	7.00	0.02	8
H03	0.92	0.04	0.42	0.03	0.46	0.03	7.00	0.04	8
H04	0.98	0.05	0.44	0.02	0.45	0.01	7.00	0.01	8
H05	0.82	0.05	0.40	0.02	0.49	0.03	6.99	0.02	8
H06	0.99	0.04	0.45	0.01	0.45	0.01	6.97	0.03	8
H07	0.95	0.06	0.43	0.02	0.45	0.01	7.00	0.01	8
H08	0.88	0.04	0.42	0.02	0.48	0.01	6.99	0.04	8
H09	0.86	0.04	0.41	0.01	0.48	0.01	7.00	0.03	8
H10	0.97	0.04	0.43	0.03	0.45	0.03	7.03	0.03	8

Note: Individual subject ^{31}P magnetic resonance spectroscopy (MRS) measurements of pH, phosphocreatine (PCr), adenosine triphosphate (γ ATP) and 'total' mobile phosphate (PCr + γ ATP + inorganic phosphorus (Pi)) ratios derived from the central eight voxels of 13 TBI patients (P1–P13) and 10 age-group-matched healthy controls (H1–H10). As part of a separate biochemical study, some patients had microdialysis catheters supplemented with either succinate or glucose, so a voxel was excluded from analysis (P01, P02, P03, P04, P05, P06, P10 and P11). Two subjects' CSI grids were positioned to capture superficially placed microdialysis catheters, excluding a further one (P06 and P09) and three (P05) voxels that represented <90% brain tissue.

correlation between brain pH measured by ^{31}P MRS and arterial blood pH measured by blood gas analyser (Spearman's $\rho = -0.61$, $p = 0.027$) (Figure 3(b)). Arterial pH ranged from 7.37 to 7.49: nine patients' results were within accepted normal physiological range (7.35–7.45), four patients were slightly alkalotic. There was no statistically significant correlation between brain pH and arterial blood PaCO_2 (Spearman's $\rho = 0.42$, $p = 0.15$) (Figure 3(c)).

We repeated the analysis with a linear mixed effects model using all ($n = 170$) voxels. This again found a statistically significant difference in PCr/ γ ATP, PCr/total-mobile-phosphate, γ ATP/total-mobile-phosphate and pH between TBI patients and healthy controls, verifying Mann-Whitney U results (Table 2, Figure 2).

There was greater variation in pH and high-energy phosphate ratios between TBI patients than between healthy controls (Table 2). The variability within each subject's eight voxels was also greater in

TBI patients (Table 3). Exploration of potential confounding variables found no correlation between pH or PCr/ γ ATP ratio and either patient age, or interval between injury and MRS scanning, nor was a difference found when patients were dichotomised into those less than or more than seven days after injury (Mann-Whitney U). Grey matter/white matter ratio was not significantly different between TBI patients and healthy controls ($p = 0.26$, Mann-Whitney), nor did it reach significance as a covariate in linear mixed model analysis of PCr/ γ ATP, PCr/total-mobile-phosphate or pH. However, it was a statistically significant covariate in linear mixed model analysis of γ ATP/total-mobile-phosphate ($p = 0.03$), and as it can affect ratios of high-energy phosphates in the healthy brain,^{14,22} it was included in all mixed effects model analysis. Inclusion of scanner type (Siemens Trio or Verio) in the mixed effects models did not affect significance.

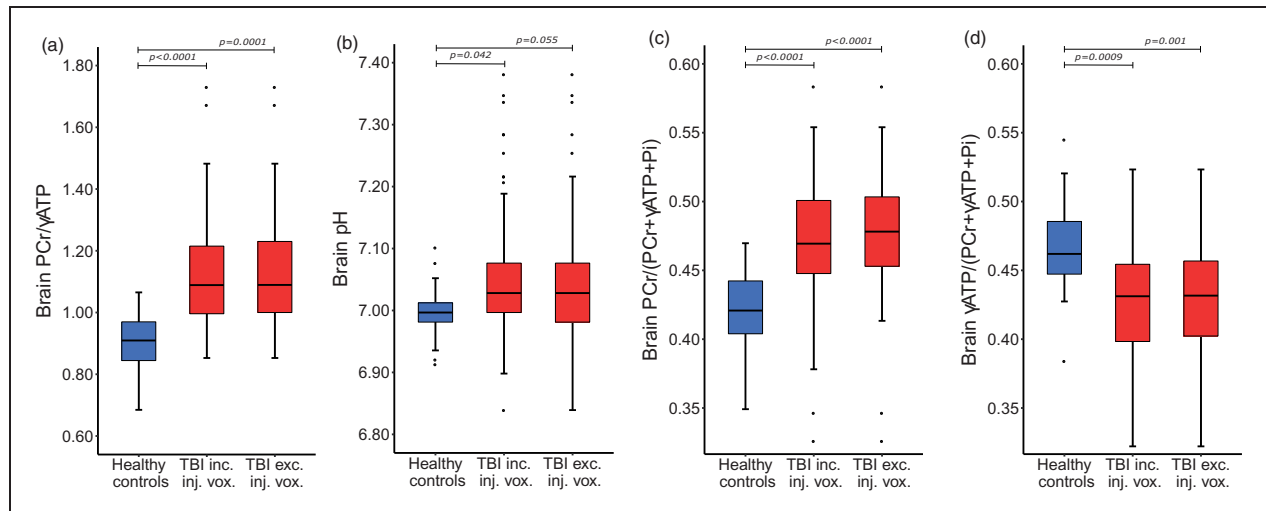


Figure 2. PCr/ γ ATP, pH, PCr/total-mobile-phosphate and γ ATP/total-mobile-phosphate changes following TBI. Box-and-whisker plots of ^{31}P magnetic resonance spectroscopy measurements in the central eight voxels of healthy controls (in blue, 80 voxels) TBI patients (in red, 90 voxels: 'TBI inc. inj. vox.'), and TBI patients after excluding voxels that contained $>5\%$ radiological injury on FLAIR or SWI sequences (in red, 73 voxels: 'TBI exc. inj. vox.'). There was a statistically significant difference in PCr/ γ ATP ratio (a), pH (b), PCr/total-mobile-phosphate (c) and γ ATP/total-mobile-phosphate (d) between TBI patients and age-group-matched healthy controls. The statistically significant differences persisted when injured voxels were excluded from analysis, except for brain pH (b, $p = 0.055$). Statistical analysis was performed using a linear mixed effects model (lme in R package nlme) that included voxel grey matter/white matter ratio as a covariate, p-values quoted in the figure. FLAIR: fluid-attenuated inversion recovery; SWI: susceptibility weighted imaging; PCr: phosphocreatine; γ ATP: adenosine triphosphate; total-mobile-phosphate: PCr + γ ATP + inorganic phosphate.

^{31}P MRS: metabolic changes by outcome

To establish whether the above changes were a marker of cellular stress and injury, or an appropriate compensatory response representing repair and recovery, we compared PCr/ATP and pH of patients with favourable outcome to those with unfavourable outcome six months after scanning using both Mann-Whitney U of subject means and linear mixed model of individual voxels. Patient outcome ranged between GOS-E-1 and GOS-E-5 and was dichotomised into favourable and unfavourable outcomes (see Materials and methods section). There was no statistically significant difference in PCr/ γ ATP between patients with favourable and unfavourable outcomes ($p > 0.2$) or PCr/total-mobile-phosphate ($p = 0.9$) by either method. There was a trend for patients with an unfavourable outcome to have a lower γ ATP/total-mobile-phosphate than patients with a favourable outcome, narrowly missing significance by Mann-Whitney U ($p = 0.051$), but significant by mixed model analysis ($p = 0.037$). Brain alkalosis (pH) was higher in patients with unfavourable outcome than patients with favourable outcome using both analytical methods ($p < 0.03$) (Table 2). Furthermore, to ascertain if the biochemical changes observed in TBI patients (relative to healthy controls) were present in both TBI outcome groups, we then included healthy controls in our model (Figure 4). Compared to healthy controls, PCr/ γ ATP and PCr/

total-mobile-phosphate was elevated in patients with favourable outcome ($p < 0.001$) and patients with unfavourable outcome ($p < 0.0001$), with no difference between the two patient groups. γ ATP/total-mobile-phosphate was lower in patients both with favourable outcome ($p = 0.048$) and unfavourable outcomes ($p < 0.0001$) compared to healthy controls, with a greater fall found in patients with unfavourable outcome ($p = 0.024$) using this method of analysis. Brain pH was found to only be alkalotic in patients with unfavourable outcome ($p = 0.0001$), and was not significantly different between patients with favourable outcome and healthy controls ($p = 0.9$). Adding healthy controls to the mixed effects model did not diminish the earlier differences that were significant between patients with favourable and unfavourable outcomes. A scatter plot of intracellular pH vs. PCr/ γ ATP with data points differentiated for healthy controls and individual GOS-E patient outcomes (Figure 5(a)) clearly shows that whilst PCr/ γ ATP elevation was a generality in patients, alkalosis was only in those with worst outcomes.

^{31}P MRS: metabolic changes in the absence of visible tissue injury

To ascertain whether brain alkalosis and elevated PCr/ γ ATP occurred generally in the traumatised brain, rather than being limited to tissue visibly injured on MRI, we repeated the data analysis excluding voxels

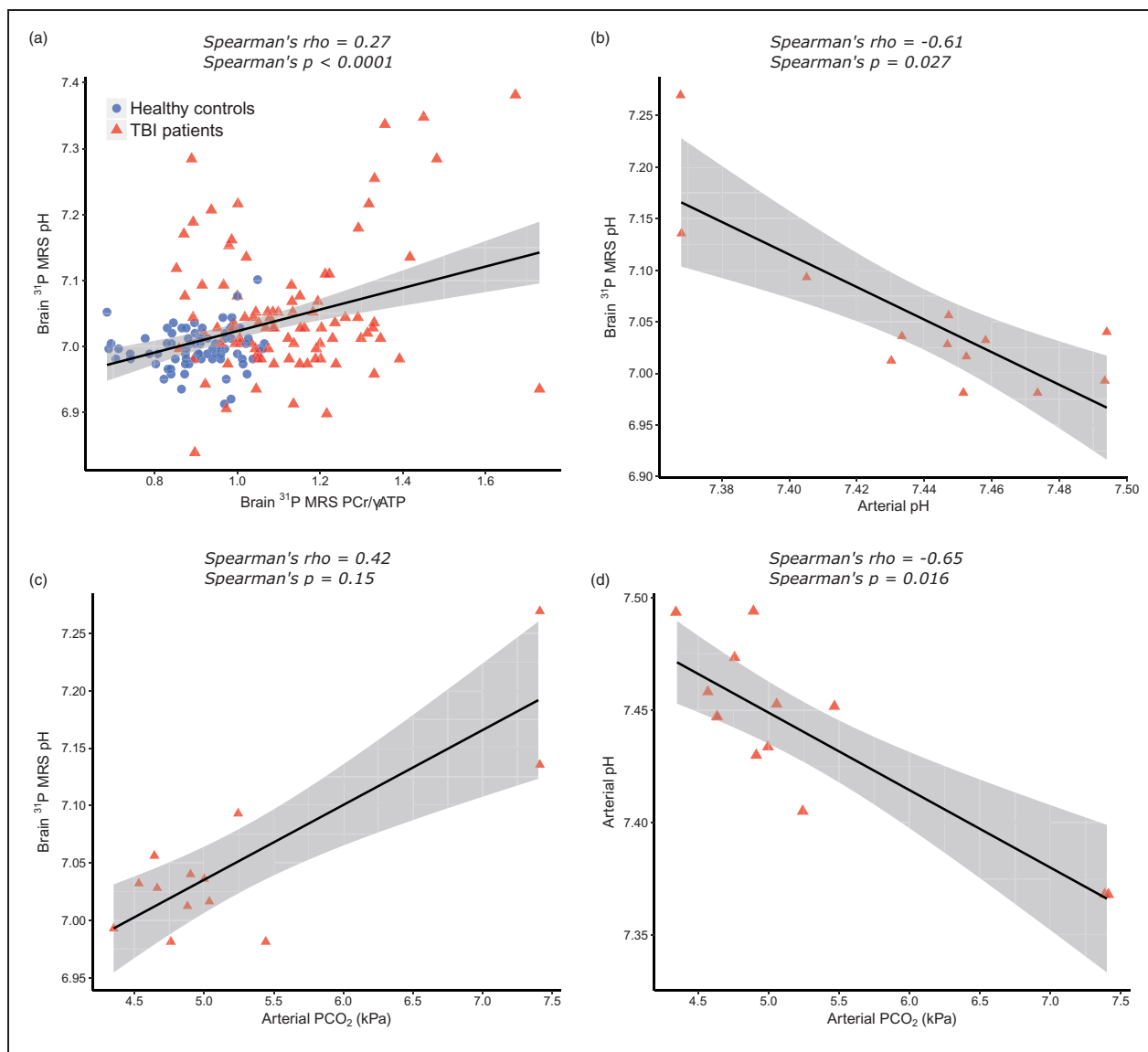


Figure 3. Scatter plots showing associations between brain pH, PCr/γATP, arterial pH and arterial PaCO₂ following TBI. (a): Brain pH and PCr/γATP ratio of combined voxels (n = 170) from healthy controls (blue circles) and TBI patients (red triangles) demonstrate a positive correlation between the two (rho = 0.27, p < 0.0001). (b): Individual patient mean brain pH, measured using ³¹P MRS, is inversely correlated with patient arterial blood pH, measured with bedside blood gas analyser (rho = -0.61, p = 0.027). (c): There was an inverse correlation between arterial pH and PaCO₂, as expected (rho = -0.65, p = 0.016). (d): there was no statistically significant relationship between arterial blood PaCO₂ and brain pH. All correlations are Spearman's ranked correlation coefficient with solid linear regression line; 95% confidence interval denoted by grey-shaded area.

with more than 5% injury on FLAIR or SWI. This revealed the same pattern, although some statistical significance weakened (see Figure 2 and Table 2): There was still a difference in within-subject mean PCr/γATP, PCr/total-mobile-phosphate and γATP/total-mobile-phosphate between all TBI patients and healthy controls by Mann-Whitney U and mixed effects model analysis (p < 0.02). The difference in pH between patients and healthy controls remained significant by

Mann-Whitney (p = 0.010), but narrowly missed significance by mixed effects model (p = 0.055). Comparing patients with favourable and unfavourable outcomes, there was still no significant difference in PCr/γATP or PCr/total-mobile-phosphate. The difference in γATP/total-mobile-phosphate narrowly lost significance, both by lme (p = 0.06) and by Mann-Whitney (p = 0.18). The difference in pH between patients with favourable outcome and unfavourable outcome

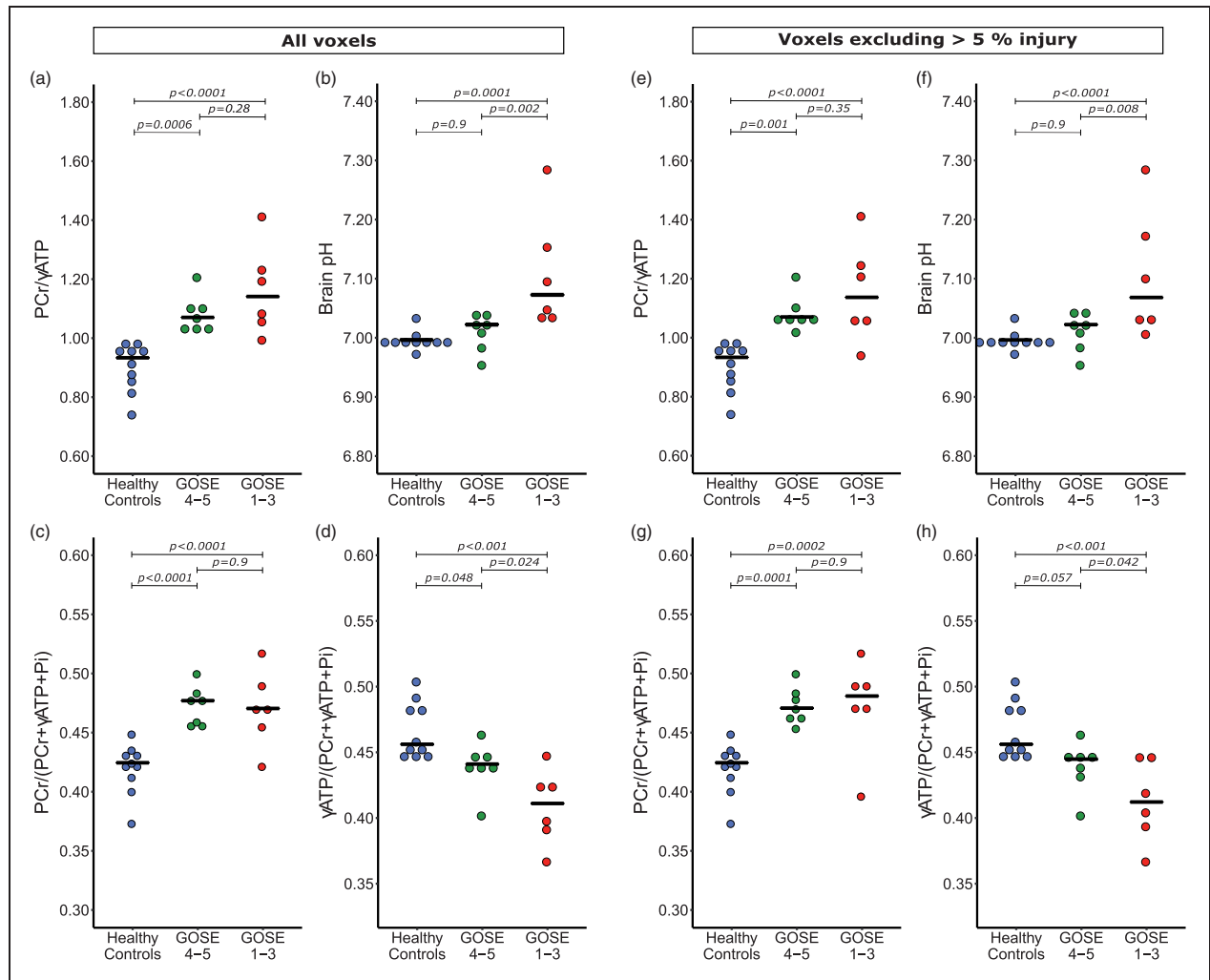


Figure 4. PCr/ γ ATP, pH, PCr/total-mobile-phosphate and γ ATP/total-mobile-phosphate changes following TBI by patient outcome – including and excluding injured voxels. Dot-plots of ^{31}P magnetic resonance spectroscopy measurements, with each point representing subject mean result, split by patient outcome at six months: healthy controls; favourable outcome (GOS-E \geq 4); and unfavourable outcome (GOS-E 1–3). (a–d) include all patient voxels, (e–h) only include voxels that contained $<$ 5% radiological injury on fluid-attenuated inversion recovery (FLAIR) or susceptibility weighted imaging (SWI) sequences. (a): PCr/ γ ATP ratio was raised in both patient groups compared to healthy controls. (b): brain pH was significantly higher in patients with an unfavourable outcome than healthy controls and patients with a favourable outcome, who did not observe a change in their brain pH. (c): PCr/total-mobile-phosphate ratio was elevated in both patient outcome groups equally. (d): γ ATP/total-mobile-phosphate ratio was significantly lower in TBI patients potentially scaled to outcome, with a lower γ ATP/total-mobile-phosphate ratio being found in patients with a worse outcome. After excluding voxels with \geq 5% injury on FLAIR and SWI sequences, the statistical significance remained with differences in PCr/ γ ATP ratio (e), brain pH (f) and PCr/total-mobile-phosphate ratio (g). The statistical significant difference in γ ATP/total-mobile-phosphate ratio between healthy controls and patients with a favourable outcome was narrowly lost ($p = 0.057$) (h). Statistical analysis was performed using a linear mixed model in R (package nlme) that included voxel grey matter/white matter ratio as a covariate, using generalised linear hypothesis tests (glht) with Bonferroni correction of the mixed effects model for inter-group comparisons. Statistical significance is indicated by bars in figures. PCr: phosphocreatine; γ ATP: adenosine triphosphate; total-mobile-phosphate: PCr + γ ATP + inorganic phosphate.

narrowly lost significance by Mann-Whitney ($p = 0.10$) and lme comparing only the two patient outcome groups ($p = 0.057$), but remained significant when healthy control subjects were included in the mixed effects model (Figure 4).

Discussion

We reveal significant changes in brain high-energy phosphate metabolism (elevation of PCr/ATP) and brain pH (alkalosis) in acute-phase major TBI patients,

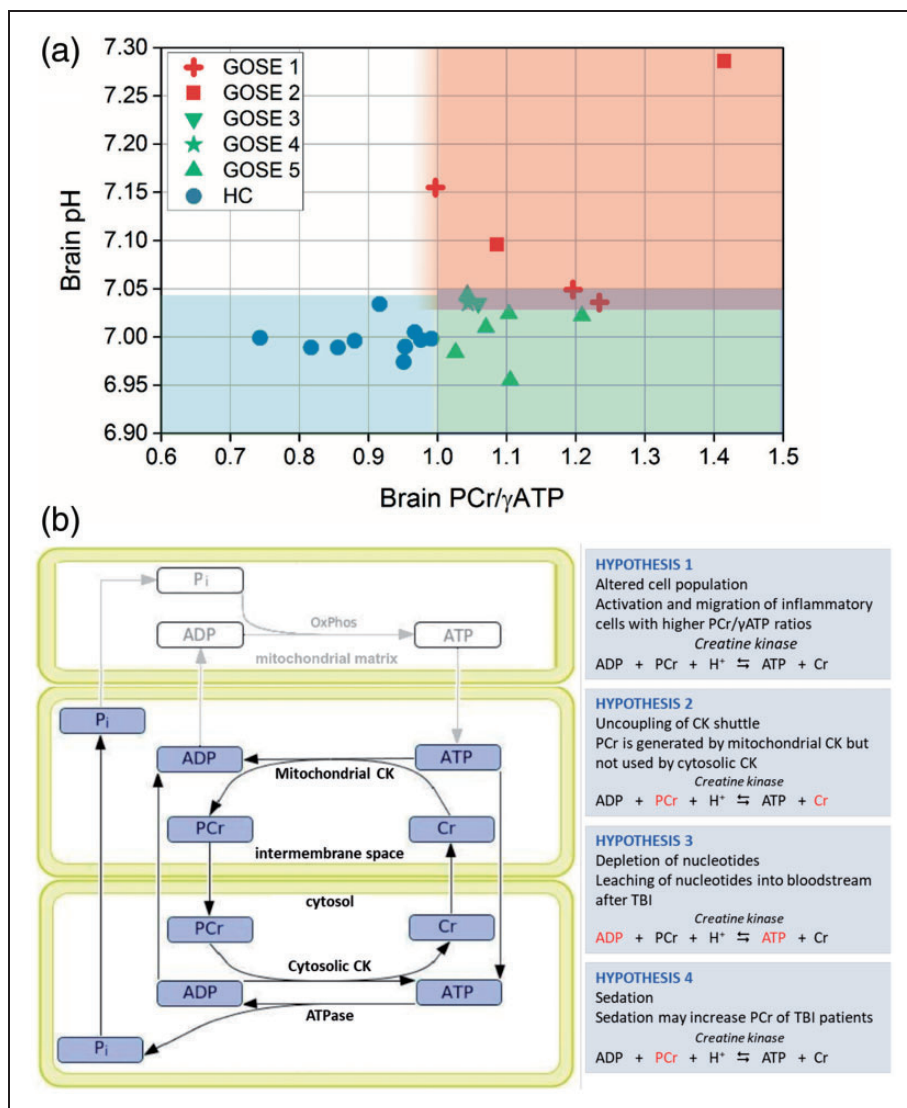


Figure 5. Hypotheses as possible explanations of our ^{31}P MRS results, and scatter plot showing relationship between brain PCr/ATP, pH and patient outcome. (a): Scatter plot of intracellular pH vs. PCr/γATP, with data points differentiated for healthy controls and patients' GOS-E outcome scores. Each data point represents the mean values for one subject. (b): hypotheses for changes observed in our sedated TBI patients, that may coincide with each other. The schematic of the compartmentalised creatine kinase system is adapted from Hettling and van Beek (2011, PLoS Comput Biol 7(8): e1002130, published Open Access © the Authors). ADP: adenosine diphosphate; ATP: adenosine triphosphate; Cr: creatine; CK: creatine kinase; PaCO₂: arterial partial pressure of CO₂; PCr: phosphocreatine; Pi: inorganic phosphate.

which appear to be related to clinical outcome. These differences persist when we excluded voxels containing structural abnormalities on MRI sequences sensitive for detecting injury following TBI – suggesting fundamental changes in energy state and acid–base balance occur in both visibly injured, and radiologically ‘uninjured’ acutely traumatised brain. Increases in patients' PCr/ATP appear driven by changes in both PCr (rise in PCr/total-mobile-phosphate) and ATP (fall in ATP/total-mobile-phosphate) – but it is unclear whether these represent a single joint phenomenon, or two independent processes. Our findings contrast

with the expectation of a low PCr/ATP ratio seen in animal studies of acute TBI,²³ and an expectation of brain ‘acidosis’ reported extracellularly in acute TBI patients^{24,25} and intracellularly in hyper-acute animal TBI models.^{23,26} However, they are consistent with changes found in the subacute/chronic phase of TBI in humans,²⁷ and sub-acutely after severe injury in rodent TBI models.^{23,26} Therefore, a high brain PCr/ATP and pH are not only recovery phase abnormalities of biochemistry, but are present in the acute phase of secondary injury after trauma. We hypothesise several explanations (Figure 5(b)), discussed below.

Change in PCr/ATP energy state following TBI

Quantification of absolute metabolite concentrations using in vivo ^{31}P MRS is challenging, and thus the PCr/ATP ratio is typically used to characterise cellular energy state. A high PCr/ATP ratio is interpreted as a tissue possessing greater energy reserve due to the relative abundance of the energy-replenishing PCr species relative to the active ATP species.²⁸ Conventionally, when ATP synthesis is running normally, the cell's PCr store is well stocked; when ATP synthesis is struggling to meet demand, the PCr store runs down.

The higher PCr/ATP in acute phase TBI, at face value, implies a 'better-stocked' store of energy in patients than controls, which might seem counter-intuitive given findings of other studies of adverse brain metabolism following major TBI: including metabolic rate of glucose,²⁹ extracellular L/P ratio² and ^{31}P MRS experimental TBI models in animals.³⁰ Indeed, findings of animal studies hyper-acutely after experimental injury showed decreased PCr with unchanging ATP (therefore lower PCr/ATP ratio),^{23,26,30} whereas we found high PCr/total-mobile-phosphate and low ATP/total-mobile-phosphate suggesting that both an increase in PCr and a fall in ATP occurred in our TBI patients' brains.

The high PCr/ATP and PCr/total-mobile-phosphate in our TBI patients may be due to a change in the brain's cell population (Hypothesis 1 in Figure 5(b)). A neuroinflammatory cascade occurs after major TBI, with proliferation and migration of glia and inflammatory cells, e.g. macrophages.³¹ Maturation and activation of macrophages increase their PCr concentration, producing a PCr 'reservoir' not seen in non-activated monocytes in the circulation.³² Glia possess a naturally higher PCr/ATP ratio than neurons^{33,34} and reserve capacity for ATP generation by increasing glycolysis of glycogen stores, or through autophagy.³⁴⁻³⁸ A higher PCr/ATP ratio (relative to healthy controls) was reported in white matter in the subacute period following TBI, attributed to glial proliferation ('reactive gliosis').²⁷ We propose that such upregulation of resident glial metabolism and activation and migration of inflammatory cells with higher PCr/ATP ratios, either from the bloodstream or through activation of resident microglia, are the most important contributors to the elevated PCr/ATP ratio in our study.

The rise in PCr/ATP and fall in ATP/total-mobile-phosphate may also represent a degree of neural tissue energy failure occurring independently of brain cell population changes and/or glial activation (Hypothesis 2, Figure 5(b)). Mammalian cells work hard to maintain ATP homeostasis, even when stressed,³⁹⁻⁴¹ so the apparent fall in ATP implied by a lower ATP/total-mobile-phosphate indicates more

extreme metabolic dysfunction, and is most evident in patients with unfavourable outcomes. The high PCr/total-mobile-phosphate we found is surprising, as PCr would be expected to regenerate ATP. However, elevated PCr/ATP may represent a combined result from two different cell populations in the traumatised brain: cells that are more sensitive to injury, such as neurons, experiencing energy failure with low ATP; and activated glia more resistant to injury, and inflammatory cells which may have a relatively higher concentration of PCr. Such concept of differentially viable cellular moieties was proposed in a subacute study of large-territory stroke,⁴² which may share similar pathophysiology with patients who have sustained a major traumatic injury. Additionally, leaching of adenine bases from the injured brain^{43,44} may contribute to the finding of low ATP together with elevated PCr; as if high-energy phosphates were generated in the absence of sufficient adenine bases, the CK equilibrium may be shifted to a higher PCr/ATP ratio. However, we regard this explanation less likely, as we would not expect selective ATP loss without loss of PCr and Cr from the traumatised brain.

Uncoupling of the mitochondrial-cytosolic CK system (Hypothesis 3 in Figure 5(b)) may also contribute to high PCr/ATP in TBI patients. PCr is synthesised in the mitochondrial inter-membrane space by octameric mitochondrial CK (Mi-CK), and used in the cytosol by the dimeric, cytosolic form of CK (BB-CK). If TBI causes greater disruption or injury to cerebral BB-CK than to Mi-CK, or disruption of PCr and Cr shuttling between the two in the cytosol and mitochondria, PCr may be produced but not used, resulting in elevated PCr/ATP from accumulation of PCr and consumption of ATP. Although PCr (211 Da) is regarded as readily diffusible in cells due to its size and charge,^{7,8} the restricted diffusion of a similar sized molecule, N-acetylaspartate (NAA, 175 Da), has been demonstrated in animal models of pathology,⁴⁵ and has more recently been demonstrated in human pathology.⁴⁶ Gabr et al. reported in an advanced ^{31}P MR diffusion spectroscopy study of human skeletal muscle that 'In a time equal to the half-life of PCr in the CK reaction, PCr would diffuse an average distance of approximately 66 micrometres'.⁴⁷ Although we could not find literature on such measurements in brain, we consider PCr as a diffusible, spatial buffer of energy reserve.

Unlike TBI, mitochondrial diseases showed below-normal PCr/ATP ratios in brains⁴⁸ and heart muscle.^{28,49} Also, physiological adaptation (rather than disease) can give 'below-normal' PCr/ATP ratios, e.g. Sherpa heart muscle.⁵⁰ In epilepsy, ipsilateral depression of PCr/ATP ratio occurred in the epileptogenic hippocampus, relative to contralateral 'healthier' hippocampus.⁵¹ Like TBI, elevated brain PCr/ATP ratios (above

healthy controls) were reported in Parkinson's disease,⁵² and in normal-appearing white matter in multiple sclerosis, attributed to diminished creatine kinase B activity.⁵³ This supports the idea that inflammation in TBI brain might at least partly contribute to the elevated PCr/ATP ratio observed.

Brain alkalosis following TBI

In the acute phase of TBI, patients' brains overall were more alkaline compared to healthy controls. Sub-group analysis revealed this to be limited to patients who had unfavourable outcomes six months later (Figure 4). ³¹P MRS measures predominantly intracellular pH,⁵⁴ estimated to represent 80% of total brain volume.^{55,56} Of this, we are likely detecting a composite of cytosolic and mitochondrial pH, as the Pi peaks from each pool do not appear separately resolved in our in vivo MRS. Extracellular acidification, measured with intracranial probes, is associated with metabolic derangement and increased TBI patient mortality.^{24,25} Intracellular acidification is seen in rodent ³¹P MRS studies of hyperacute major TBI,⁵⁷ followed by a period of intracellular alkalosis.²⁶ A ³¹P MRS study of recovering patients in the subacute/chronic phase of TBI found (intracellular) alkalosis of patients' white matter.²⁷ Our finding of brain intracellular alkalosis in acute-phase TBI patients with unfavourable outcome six months later suggests that acute-phase alkalosis occurs when physiology is severely deranged, rather than simply being a feature of recovery after injury. Brain alkalosis was found experimentally in rats 24–48 h after transient (8 min) forebrain ischaemia followed by reperfusion.⁵⁸ In a clinical ³¹P MRS study of large-territory ischaemic stroke, hyper-acute brain acidification was reported (within 18 h of infarct), followed by brain alkalosis (by day 3) which persisted for 29 days¹³; these findings are supported by a later study of stroke patients 3–12 days after ictus.⁴² Infarction is an extreme tissue injury, so concurs with our finding of brain alkalosis in TBI patients who proceed to unfavourable outcomes – although our study demonstrates alkalosis in normal-appearing tissue on conventional and advanced MR imaging.

The interrelationships among intracellular pH, extracellular pH, and their biological implications are complex and incompletely understood. Mammalian cells strive to maintain an optimal intracellular pH and actively transport H⁺ ions extracellularly by several regulatory mechanisms, as they can only survive when intracellular pH is neutral or slightly alkaline.^{59,60} When astrocytes become alkalotic, their rate of glycolysis increases, likely through increased activity of the rate-limiting enzyme phosphofructokinase with an optimum around pH 7.2–7.3, and a steep pH dependence,

falling dramatically at lower pH.^{61,62} Astrocyte glycolysis produces lactate; each lactate anion is co-transported by monocarboxylate transporters out of the cell accompanied by an H⁺ ion⁵⁹ to 'feed' neurons in the model of the astrocyte-neuron lactate shuttle hypothesis.^{63,64} Upregulation of brain glycolytic activity was shown in acute severe TBI.^{2,4,65,66} If an increase in astrocytic lactate/H⁺ export was not matched by increased lactate/H⁺ uptake by neurons, extracellular acidosis would occur in the presence of intracellular alkalosis. Given the greater vulnerability of neurons compared to glia, this may explain the intracellular alkalosis we see, and the extracellular acidosis in other reports.^{25,67}

Glial alkalosis may be self-regulated, or driven by neurons. Astrocytes can adapt their intracellular pH 'set-point' to be more alkaline,⁶⁸ which increases their rate of glycolysis and synthesis of protein, DNA and RNA. This occurs in astrocytic tumours for cell division,^{59,69} and conceivably also for cellular repair in injured astrocytes. Several mechanisms regulate pH in astrocytes.⁵⁹ Intracellular alkalosis may arise from the cell exporting H⁺ ions – including those generated by glycolysis. This may be via monocarboxylate transporters (see above) that do not consume ATP. However, another H⁺-extrusion pathway is via H⁺-ATPase pumps that directly consume ATP. If this were necessary for cells to maintain glycolysis, it may significantly reduce the net efficiency of glycolytic ATP production if mitochondrial function were impaired in the traumatised brain,^{2,70} as only two moles of ATP per mole of glucose are produced by 'isolated glycolysis'. If NADH shuttling (e.g. malate-aspartate shuttle) from the cytosol into mitochondria is operational then further ATP molecules can ensue from glycolysis. The yield per mole of glucose metabolised fully to CO₂ (by the combination of glycolysis, NADH shuttling and mitochondrial respiration) is theoretically 36–38 moles of ATP. However, the actual yield is considered somewhat lower.^{71,72} Upregulation of astrocyte glycolysis by intracellular alkalosis may also be activated by local neurons, as glial cytosolic alkalosis occurs in response to local neuronal activity.^{73,74} In TBI this may be a purposeful mechanism for neurons to induce additional metabolic support; or be a pathophysiological consequence of neuronal glutamate excitotoxic injury, associated with leakage of cytoplasmic elements from injured neurons.^{75,76}

Alkali brain pH appears distinctive for patients who emerged with the worst clinical outcomes, concurring with the association between brain hyperglycolytic state and TBI mortality.⁶⁵ This implies that after TBI, alkalosis is either caused by energy perturbation proceeding in the worst cases to an adaptive state of alkaline pH associated with abnormal cell biology and biochemistry, or that alkalosis is a distinct product of more

catastrophic neuronal injury. The significant change in pH in patients with unfavourable outcome, with no change in patients with favourable outcome suggests that sedation did not affect brain pH, as all patients were treated effectively similarly.

A change in cell population, a proposed explanation for the elevation in PCr/ATP (see above), may also contribute to brain alkalinisation. White matter alkalosis was attributed to reactive gliosis because regions of pathology containing more glial cells (e.g. low-grade astrocytomas) typically have a higher pH.²⁷ Reactive gliosis may thus contribute to elevation of both pH and PCr/ATP in our study.

Possible effects of sedation

Anaesthetising patients with propofol and midazolam sedation might have influenced our findings in TBI patients (Hypothesis 4, Figure 5(b)). Powerful sedatives such as pentobarbitone (pentobarbital)⁷⁷ and high doses of diethyl ether, phenobarbital and sodium thiopentone⁷⁸ increased cerebral PCr in rodents (assayed biochemically after extraction, not MRS). Conversely, light sedatives and analgesics had no effect on rat brain PCr concentration, and no sedative/anaesthetic agents (at any concentration) influenced cerebral ATP concentration in those studies.^{39,77,78} Pentobarbitone also decreased the TCA cycle rate in rats.⁷⁹ Brain pH was not reported in those anaesthetic studies. The effects of propofol and midazolam on high-energy phosphates are unknown, but might resemble those of pentobarbitone and sodium thiopentone more than those of light sedation and analgesia. The elevation of PCr/total-mobile-phosphate was equivalent across our TBI outcome groups, so might be due to sedation. However, sedation/anaesthesia would not explain changes in ATP/total-mobile-phosphate (and pH, discussed below), as this decreased more in patients with unfavourable outcome, and all patients were treated essentially the same. Moreover, no changes in ATP were reported in the rodent sedation studies,^{39,77,78} and changes in PCr/ATP and pH were reported in subacute TBI patients, including those mechanically ventilated (without barbiturates, but presumably sedated) and those self-ventilating.²⁷ Thus, although sedation may have influenced the changes in high-energy phosphates that we observe, it is probably less important than the effect of brain injury in accounting for differences in high-energy phosphates and pH in our study. Interestingly, brain PCr/ATP and pH both increased in a ³¹P MRS study of experimental (sheep) hypothermia.⁸⁰ Although we did not use hypothermia, parallels may exist with TBI if ATP synthesis is faster than its utilisation and unused ATP increasingly transfers its high-energy phosphate energy potential to the PCr store.

Ventilation and alkalosis

Increasing ventilation to lower PaCO₂ can cause brain alkalosis, as shown by ³¹P MRS in self-hyperventilating healthy volunteers.⁸¹ In mechanically hyperventilated TBI patients, intracranial probes detected *extracellular* alkalosis.⁸² However, our TBI management protocol maintains arterial PaCO₂ > 4 kPa, and the mean PaCO₂ of our TBI patients was 4.8 kPa (range 4.3–7.4 kPa), equivalent to that expected in healthy subjects breathing normally. Interestingly, brain pH correlated inversely with arterial pH, apparently driven by arterial PaCO₂ (Figure 3). Brain alkalosis was absent in our ventilated patients with favourable outcome who received similar treatment during MRS. Brain alkalosis was reported in TBI patients' white matter in both self-ventilating and mechanically ventilated TBI patients sub-acutely post-injury.²⁷

Metabolic derangement in radiologically normal-appearing brain

When we excluded voxels with ≥5% radiological injury, the pattern of elevated PCr/ATP and elevated pH persisted in TBI brain (Figure 2), suggesting diffuse metabolic derangement throughout the brain. The difference in brain pH between all TBI patients and healthy controls was narrowly lost statistically, attributable to lower 'n' and the absence of change in patients with a favourable outcome 'diluting' the effect seen in patients with unfavourable outcome. Reported using ¹H MRS six months post-TBI, the marker of neuronal integrity and density NAA/Cr was lower, and the cell turnover marker Cho/Cr higher in radiologically-normal-appearing brain, with the magnitude of change predicting patient outcome.⁸³ Similar ¹H MRS findings in another study appeared unrelated to abnormalities on conventional MR sequences.⁶⁶ In the chronic phase of TBI, abnormalities were reported using ¹H MRS in radiologically-normal-appearing patients' thalami,⁸⁴ frontal cortex⁸⁵ and occipito-parietal cortex.⁸⁶ Our ³¹P MRS findings of early metabolic abnormality in radiologically-normal-appearing brain after major TBI thus concur with previous ¹H MRS reports, supporting the concept that microscopic whole-brain injury following TBI extends beyond macroscopic MRI-visible abnormalities.

³¹P MRS and clinical outcome

The relationship between the changes we observe in brain ³¹P MRS biochemistry and patient outcome suggests these changes represent underlying pathophysiology of brain injury, and that ³¹P MRS may be an

early predictor of six-month outcome after major TBI. Patient outcome may correlate with some aspects of MRI-visible structural injury,⁸⁷ but MRI-visible injury is unreliable alone as a predictor⁸⁸ because of microscopic tissue damage without radiologically identifiable injury.^{83,88,89} ¹H MRS characteristics of 'microscopic' tissue injury were identified acutely and sub-acutely after injury that correlate with clinical outcome⁶⁶: recovery of NAA,⁹⁰ NAA/Cr in the corpus callosum,⁹¹ and NAA/Cr in the brainstem.⁹² Our study is the first to demonstrate that acute-phase changes measured by ³¹P MRS relate to clinical outcomes six months later. Brain alkalosis only occurred in patients with ultimately unfavourable outcomes. Importantly, this remained true when injured voxels were excluded, suggesting ³¹P MRS utility in addition to ¹H MRS structural imaging. Of the three patients with unfavourable outcome and severe brain alkalosis (P03, P04, P05), their predicted risks of unfavourable outcome at six months were respectively 31%, 74% and 86%, on the CRASH head injury prognosis calculator (Supplementary Table 2),⁹³ suggesting that patient P03 suffered metabolic injury unapparent to current predictive models. Early warning from ³¹P MRS measurement of alkalosis that a patient may be heading towards unfavourable outcome will maximise opportunity for intervention to improve outcome. Furthermore, patient P02 *without* pronounced brain alkalosis emerged with favourable (GOS-E 5) outcome, despite CRASH prediction of 90% risk of unfavourable outcome. Although PCr/ATP did not reliably discriminate between TBI patient outcome groups, ATP/total-mobile-phosphate was lower in patients with unfavourable outcome than patients with favourable outcome. Again, this persisted when radiologically injured voxel data were excluded (Figure 4). ³¹P MRS may thus help early recognition of patients who will emerge better than conventionally predicted. Our promising findings merit further, larger studies to confirm these relationships between acute ³¹P MRS and 6-month outcome, and determine whether the technique might augment existing (non-MRS) outcome prognostication.⁹³

Strengths and limitations

³¹P comprises 100% of all naturally occurring phosphorus atoms, so artificial enrichment is unnecessary for MR, which is non-invasive. Due to technical constraints of in vivo MRS, absolute quantification of concentrations is very difficult to achieve accurately, so we used PCr/ATP ratio; enabling reliable comparisons for statistical analysis. For good sensitivity within a practicable scan duration, we used $2.5 \times 2.5 \times 2.5$ cm³ voxels. The central eight voxels were chosen as they

represented a large volume of subjects' brains, whilst avoiding signal contamination from bone, muscle and scalp. Only 17 central eight voxels contained >5% injury, too few for meaningful subgroup statistical analysis.

In vivo MRI/MRS of sedated, ventilated patients in the acute phase of secondary brain injury following major TBI is challenging, and ³¹P MRS, although non-invasive, safe, and not excessive on scan time, is not yet routinely used. Our promising results in this small cohort (13 patients, 10 controls) merit larger studies, including uninjured anaesthetised brain, to elucidate fundamental biochemical abnormalities following major TBI and establish the prognostic power of acute-phase ³¹P MRS.

Conclusions

Here we have shown that clinical in vivo ³¹P MRS reveals significant changes in brain high-energy phosphate metabolism acutely after major TBI, indicating that a change in brain energy state accompanies known changes in brain metabolism.² The higher energy-store status (PCr/ATP) found in TBI patients compared to healthy controls is perhaps surprising, given the conventional view of 'energy crisis' in TBI, but appears to be due to both a relative increase in PCr and a relative fall in ATP, within the combined pool of total-mobile-phosphate. Among various hypotheses, upregulation of resident microglia and migratory influx of inflammatory cells with higher PCr/ATP ratio are likely, with possible variation in energy status dependent on the cell type and susceptibility to injury. Acute TBI and inflammation are usually regarded as associated with (extracellular) 'acidosis', but we show for the first time that brain (intracellular) alkalosis occurs in the acute phase of TBI. This appears limited to patients who emerge with unfavourable outcome after six months, suggesting acute-phase raised intracellular pH is important pathophysiologically in TBI. These changes in PCr/ATP and pH are present in radiologically normal, 'uninjured' tissue on MR sequences sensitive for injury, suggesting widespread metabolic derangement occurs throughout the brain after major TBI, not just in lesions. Although we primarily used patient outcome to help understand these biochemical changes, brain pH shows potential as an early predictor of patient outcome after major TBI. No patient with a mean brain pH ≥ 7.05 had a favourable outcome. Combining voxel-based ³¹P MRS brain pH measurement with existing predictive TBI outcome models may improve accuracy. Further study of ³¹P MRS in TBI is merited to explore its full potential in evaluating brain injury, response to therapy, and how these correlate with outcome.

Funding

The author(s) disclosed receipt of the following financial support for the research, authorship and/or publication of this article: Medical Research Council (Grant Nos. G0600986 ID79068 and G1002277 ID98489) and National Institute for Health Research Biomedical Research Centre, Cambridge (Neuroscience Theme; Brain Injury and Repair Theme). Authors' support: MGS and SGC – National Institute for Health Research Biomedical Research Centre, Cambridge; MOM – Medical Research Council (MR/N025792/1); IJ – Medical Research Council (Grant no. G1002277 ID 98489) and National Institute for Health Research Biomedical Research Centre, Cambridge; KLHC – National Institute for Health Research Biomedical Research Centre, Cambridge (Neuroscience Theme; Brain Injury and Repair Theme); CG – the Canadian Institute of Health Research; AH – Medical Research Council/Royal College of Surgeons of England Clinical Research Training Fellowship (Grant no. G0802251), Royal College of Surgeons of England Pump Priming Grant and the National Institute for Health Research Biomedical Research Centre, Cambridge; DKM – National Institute for Health Research Senior Investigator Awards; PJH – National Institute for Health Research (NIHR) Research Professorship, Academy of Medical Sciences/Health Foundation Senior Surgical Scientist Fellowship and the National Institute for Health Research Biomedical Research Centre, Cambridge. MPM – Medical Research Council UK (MC_U105663142) and a Wellcome Trust Investigator award (110159/Z/15/Z).

Acknowledgements

We thank Christopher Randell (PulseTeq Ltd) for custom-building the ^{31}P head-coil and for advice on ^{31}P MRS, and Prof. John D. Pickard for his advice and support setting up the study. We thank the Anaesthetic Research Fellows and Anaesthetic Research Nurses for their assistance taking patients for MR scans, and we gratefully thank the patients and the healthy controls for participating in this study, and the patients' relatives for their assent.

Declaration of conflicting interests

The author(s) declared no potential conflicts of interest with respect to the research, authorship, and/or publication of this article.

Authors' contributions

The study concept was by PJA, DKM, KLHC, AH, TAC, MPM and CNG. The study design was by MGS, KLHC, TAC and AH. MGS, MOM, IJ, DJH, PG and AM performed the experimental work. MGS, JLY, MRG, AH, IJ, MOM, KEW, MPM, DKM, KLHC and PJA assessed and analysed the data. MGS, KLHC, DKM and PJA wrote the manuscript. All authors reviewed and edited the manuscript.

Supplementary material

Supplementary material for this paper can be found at the journal website: <http://journals.sagepub.com/home/jcb>

ORCID iD

Matthew G Stovell  <http://orcid.org/0000-0002-4172-4617>

References

1. Maas AIR, Menon DK, Adelson PD, et al. Traumatic brain injury: integrated approaches to improve prevention, clinical care, and research. *Lancet Neurol* 2017; 16: 987–1048.
2. Timofeev I, Carpenter KLH, Nortje J, et al. Cerebral extracellular chemistry and outcome following traumatic brain injury: a microdialysis study of 223 patients. *Brain* 2011; 134: 484–494.
3. Timofeev I, Czosnyka M, Carpenter KLH, et al. Interaction between brain chemistry and physiology after traumatic brain injury: impact of autoregulation and microdialysis catheter location. *J Neurotrauma* 2011; 28: 849–860.
4. Carpenter KLH, Jalloh I and Hutchinson PJ. Glycolysis and the significance of lactate in traumatic brain injury. *Front Neurosci* 2015; 9: 112.
5. Nordström CH, Nielsen TH, Schälén W, et al. Biochemical indications of cerebral ischaemia and mitochondrial dysfunction in severe brain trauma analysed with regard to type of lesion. *Acta Neurochir (Wien)* 2016; 158: 1231–1240.
6. Williamson DH, Lund P and Krebs HA. The redox state of free nicotinamide-adenine dinucleotide in the cytoplasm and mitochondria of rat liver. *Biochem J* 1967; 103: 514–527.
7. Wallimann T, Tokarska-Schlattner M and Schlattner U. The creatine kinase system and pleiotropic effects of creatine. *Amino Acids* 2011; 40: 1271–1296.
8. Schlattner U, Tokarska-Schlattner M and Wallimann T. Mitochondrial creatine kinase in human health and disease. *Biochim Biophys Acta* 2006; 1762: 164–180.
9. Menon DK and Ercole A. Critical care management of traumatic brain injury. *Handb Clin Neurol* 2017; 140: 239–274.
10. Jennett B, Snoek J, Bond MR, et al. Disability after severe head injury: observations on the use of the Glasgow Outcome Scale. *J Neurol Neurosurg Psychiatry* 1981; 44: 285–293.
11. Maas AIR, Murray GD, Roozenbeek B, et al. Advancing care for traumatic brain injury: findings from the IMPACT studies and perspectives on future research. *Lancet Neurol* 2013; 12: 1200–1210.
12. Hutchinson PJ, Koliás AG, Timofeev IS, et al. Trial of decompressive craniectomy for traumatic intracranial hypertension. *N Engl J Med* 2016; 375: 1119–1130.
13. Levine SR, Helpert JA, Welch KM, et al. Human focal cerebral ischemia: evaluation of brain pH and energy metabolism with P-31 NMR spectroscopy. *Radiology* 1992; 185: 537–544.
14. Mason GF, Chu W-J, Vaughan JT, et al. Evaluation of ^{31}P metabolite differences in human cerebral gray and white matter. *Magn Reson Med* 1998; 39: 346–353.
15. de Graaf RA. *In vivo NMR spectroscopy*, 2nd ed. Chichester, UK: John Wiley & Sons, Ltd, 2007.

16. Stubbs M, Freeman D and Ross BD. Formation of N.M.R.-invisible ADP during renal ischaemia in rats. *Biochem J* 1984; 224: 241–246.
17. Takami H, Furuya E, Tagawa K, et al. NMR-invisible ATP in rat heart and its change in ischemia. *J Biochem* 1988; 104: 35–39.
18. Prichard JW and Shulman RG. NMR spectroscopy of brain metabolism in vivo. *Annu Rev Neurosci* 1986; 9: 61–85.
19. Petroff OA, Prichard JW, Behar KL, et al. Cerebral intracellular pH by ³¹P nuclear magnetic resonance spectroscopy. *Neurology* 1985; 35: 781–788.
20. Stovell MG, Mada MO, Helmy A, et al. The effect of succinate on brain NADH/NAD⁺ redox state and high energy phosphate metabolism in acute traumatic brain injury. *Scientific Reports* 2018; 8: 11140.
21. Pinheiro J, Bates D, DebrRoy S, et al. nlme: linear and nonlinear mixed effects models, <https://cran.r-project.org/package=nlme> (2018, accessed 22 August 2018).
22. Hetherington HP, Spencer DD, Vaughan JT, et al. Quantitative ³¹P spectroscopic imaging of human brain at 4 Tesla: assessment of gray and white matter differences of phosphocreatine and ATP. *Magn Reson Med* 2001; 45: 46–52.
23. Vink R, McIntosh TK, Yamakami I, et al. ³¹P NMR characterization of graded traumatic brain injury in rats. *Magn Reson Med* 1988; 6: 37–48.
24. Gupta AK, Zygun DA, Johnston AJ, et al. Extracellular brain pH and outcome following severe traumatic brain injury. *J Neurotrauma* 2004; 21: 678–684.
25. Timofeev I, Nortje J, Al-Rawi PG, et al. Extracellular brain pH with or without hypoxia is a marker of profound metabolic derangement and increased mortality after traumatic brain injury. *J Cereb Blood Flow Metab* 2013; 33: 422–427.
26. McIntosh TK, Faden AI, Bendall MR, et al. Traumatic brain injury in the rat – alterations in brain lactate and pH as characterized by H-1 and P-31 nuclear-magnetic-resonance. *J Neurochem* 1987; 49: 1530–1540.
27. Garnett MR, Corkill RG, Blamire AM, et al. Altered cellular metabolism following traumatic brain injury: a magnetic resonance spectroscopy study. *J Neurotrauma* 2001; 18: 231–240.
28. Lodi R, Rajagopalan B, Blamire AM, et al. Cardiac energetics are abnormal in Friedreich ataxia patients in the absence of cardiac dysfunction and hypertrophy: an in vivo ³¹P magnetic resonance spectroscopy study. *Cardiovasc Res* 2001; 52: 111–119.
29. Hattori N, Huang S, Wu H, et al. Correlation of regional metabolic rates of glucose with Glasgow Coma Scale after traumatic brain injury. *J nucl Med* 2003; 44: 1709–1716.
30. Vink R, Faden AI and McIntosh TK. Changes in cellular bioenergetic state following graded traumatic brain injury in rats: determination by phosphorus 31 magnetic resonance spectroscopy. *J Neurotrauma* 1988; 5: 315–330.
31. Burda JE and Sofroniew MV. Reactive gliosis and the multicellular response to CNS damage and disease. *Neuron* 2014; 81: 229–248.
32. Loike JD, Kozler VF and Silverstein SC. Creatine kinase expression and creatine phosphate accumulation are developmentally regulated during differentiation of mouse and human monocytes. *J Exp Med* 1984; 159: 746–757.
33. Alves PM, Fonseca LL, Peixoto CC, et al. NMR studies on energy metabolism of immobilized primary neurons and astrocytes during hypoxia, ischemia and hypoglycemia. *NMR Biomed* 2000; 13: 438–448.
34. Brand A, Richter-Landsberg C and Leibfritz D. Multinuclear NMR studies on the energy metabolism of glial and neuronal cells. *Dev Neurosci* 1993; 15: 289–298.
35. Hertz L, Peng L and Dienel GA. Energy metabolism in astrocytes: high rate of oxidative metabolism and spatiotemporal dependence on glycolysis/glycogenolysis. *J Cereb Blood Flow Metab* 2007; 27: 219–249.
36. Hertz L, Xu J, Song D, et al. Astrocytic glycogenolysis: mechanisms and functions. *Metab Brain Dis* 2015; 30: 317–333.
37. Glick D, Barth S and Macleod KF. Autophagy: cellular and molecular mechanisms. *J Pathol* 2010; 221: 3–12.
38. Falkowska A, Gutowska I, Goschorska M, et al. Energy metabolism of the brain, including the cooperation between astrocytes and neurons, especially in the context of glycogen metabolism. *Int J Mol Sci* 2015; 16: 25959–25981.
39. Sauter A and Rudin M. Determination of creatine kinase kinetic parameters in rat brain by NMR magnetization transfer: correlation with brain function. *J Biol Chem* 1993; 268: 13166–13171.
40. Prichard JW, Alger JR, Behar KL, et al. Cerebral metabolic studies in vivo by ³¹P NMR. *Proc Natl Acad Sci* 1983; 80: 2748–2751.
41. Petroff OA, Prichard JW, Behar KL, et al. In vivo phosphorus nuclear magnetic resonance spectroscopy in status epilepticus. *Ann Neurol* 1984; 16: 169–77.
42. Zöllner JP, Hattingen E, Singer OC, et al. Changes of pH and energy state in subacute human ischemia assessed by multinuclear magnetic resonance spectroscopy. *Stroke* 2015; 46: 441–446.
43. zur Nedden S, Doney AS and Frenguelli BG. The double-edged sword: gaining adenosine at the expense of ATP. How to balance the books. In: Masino S and Boison D (eds) *Adenosine*. New York, NY: Springer New York, 2012, pp.109–129.
44. Weigand MA, Michel A, Eckstein HH, et al. Adenosine: a sensitive indicator of cerebral ischemia during carotid endarterectomy. *Anesthesiology* 1999; 91: 414–421.
45. Nicolay K, Braun KP, Graaf RA, et al. Diffusion NMR spectroscopy. *NMR Biomed* 2001; 14: 94–111.
46. Wood ET, Ronen I, Techawiboonwong A, et al. Investigating axonal damage in multiple sclerosis by diffusion tensor spectroscopy. *J Neurosci* 2012; 32: 6665–6669.
47. Gabr RE, El-Sharkawy A-MM, Schär M, et al. High-energy phosphate transfer in human muscle: diffusion of phosphocreatine. *Am J Physiol Cell Physiol* 2011; 301: C234–C241.
48. Eleff SM, Barker PB, Blackband SJ, et al. Phosphorus magnetic resonance spectroscopy of patients with

- mitochondrial cytopathies demonstrates decreased levels of brain phosphocreatine. *Ann Neurol* 1990; 27: 626–630.
49. Bates MGD, Hollingsworth KG, Newman JH, et al. Concentric hypertrophic remodelling and subendocardial dysfunction in mitochondrial DNA point mutation carriers. *Eur Heart J Cardiovasc Imaging* 2013; 14: 650–658.
 50. Hochachka PW, Clark CM, Holden JE, et al. 31P magnetic resonance spectroscopy of the Sherpa heart: a phosphocreatine/adenosine triphosphate signature of metabolic defense against hypobaric hypoxia. *Proc Natl Acad Sci U S A* 1996; 93: 1215–1220.
 51. Pan JW, Williamson A, Cavus I, et al. Neurometabolism in human epilepsy. *Epilepsia* 2008; 49: 31–41.
 52. Hu MT, Taylor-Robinson SD, Chaudhuri KR, et al. Cortical dysfunction in non-demented Parkinson's disease patients: a combined (31)P-MRS and (18)FDG-PET study. *Brain* 2000; 123(Pt 2): 340–352.
 53. Steen C, Wilczak N, Hoogduin JM, et al. Reduced creatine kinase B activity in multiple sclerosis normal appearing white matter. *PLoS One* 2010; 5: e10811.
 54. Ren J, Sherry AD and Malloy CR. 31 P-MRS of healthy human brain: ATP synthesis, metabolite concentrations, pH, and T 1 relaxation times. *NMR Biomed* 2015; 28: 1455–1462.
 55. Nicholson C, Kamali-Zare P and Tao L. Brain extracellular space as a diffusion barrier. *Comput Vis Sci* 2011; 14: 309–325.
 56. Syková E and Nicholson C. Diffusion in brain extracellular space. *Physiol Rev* 2008; 88: 1277–1340.
 57. Vink R, McIntosh TK, Weiner MW, et al. Effects of traumatic brain injury on cerebral high-energy phosphates and pH: a 31P magnetic resonance spectroscopy study. *J Cereb Blood Flow Metab* 1987; 7: 563–571.
 58. Chopp M, Chen H, Vande Linde AMQ, et al. Time course of postischemic intracellular alkalosis reflects the duration of ischemia. *J Cereb Blood Flow Metab* 1990; 10: 860–865.
 59. McLean LA, Roscoe J, Jorgensen NK, et al. Malignant gliomas display altered pH regulation by NHE1 compared with nontransformed astrocytes. *Am J Physiol Cell Physiol* 2000; 278: C676–C688.
 60. Chiche J, Le Fur Y, Vilmen C, et al. In vivo pH in metabolic-defective Ras-transformed fibroblast tumors: key role of the monocarboxylate transporter, MCT4, for inducing an alkaline intracellular pH. *Int J cancer* 2012; 130: 1511–1520.
 61. Trivedi B and Danforth WH. Effect of pH on the kinetics of frog muscle phosphofructokinase. *J Biol Chem* 1966; 241: 4110–4112.
 62. Theparambil SM, Weber T, Schmälzle J, et al. Proton fall or bicarbonate rise: glycolytic rate in mouse astrocytes is paved by intracellular alkalization. *J Biol Chem* 2016; 291: 19108–19117.
 63. Pellerin L and Magistretti PJ. Glutamate uptake into astrocytes stimulates aerobic glycolysis: a mechanism coupling neuronal activity to glucose utilization. *Proc Natl Acad Sci U S A* 1994; 91: 10625–10629.
 64. Bouzier-Sore A-K, Voisin P, Canioni P, et al. Lactate is a preferential oxidative energy substrate over glucose for neurons in culture. *J Cereb Blood Flow Metab* 2003; 23: 1298–1306.
 65. Glenn TC, Kelly DF, Boscardin WJ, et al. Energy dysfunction as a predictor of outcome after moderate or severe head injury: indices of oxygen, glucose, and lactate metabolism. *J Cereb Blood Flow Metab* 2003; 23: 1239–1250.
 66. Marino S, Zei E, Battaglini M, et al. Acute metabolic brain changes following traumatic brain injury and their relevance to clinical severity and outcome. *J Neurol Neurosurg Psychiatry* 2007; 78: 501–507.
 67. Zygun DA, Steiner LA, Johnston AJ, et al. Hyperglycemia and brain tissue pH after traumatic brain injury. *Neurosurgery* 2004; 55: 877–882.
 68. Swietach P, Vaughan-Jones RD, Harris AL, et al. The chemistry, physiology and pathology of pH in cancer. *Philos Trans R Soc Lond B Biol Sci* 2014; 369: 20130099.
 69. Madshus IH. Regulation of intracellular pH in eukaryotic cells. *Biochem J* 1988; 250: 1–8.
 70. DeVience SJ, Lu X, Proctor J, et al. Metabolic imaging of energy metabolism in traumatic brain injury using hyperpolarized [1-13C]pyruvate. *Sci Rep* 2017; 7: 1907.
 71. Berg JM, Jeremy M, Tymoczko JL, et al. *Biochemistry*. 5th edition. New York: W.H. Freeman, 2002.
 72. Lodish HF. *Molecular cell biology*. W.H. Freeman, www.ncbi.nlm.nih.gov/books/NBK21475/ (2000, accessed 10 June 2018).
 73. Chesler M. Regulation and modulation of pH in the brain. *Physiol Rev* 2003; 83: 1183–1221.
 74. Chesler M and Kraig RP. Intracellular pH transients of mammalian astrocytes. *J Neurosci* 1989; 9: 2011–2019.
 75. Kilinc D, Gallo G and Barbee KA. Mechanically-induced membrane poration causes axonal beading and localized cytoskeletal damage. *Exp Neurol* 2008; 212: 422–430.
 76. Farkas O, Lifshitz J and Povlishock JT. Mechanoporation induced by diffuse traumatic brain injury: an irreversible or reversible response to injury? *J Neurosci* 2006; 26: 3130–3140.
 77. Nilsson L and Siesjö BK. Influence of anaesthetics on the balance between production and utilization of energy in the brain. *J Neurochem* 1974; 23: 29–36.
 78. Nilsson L and Siesjö BK. The effect of anesthetics upon labile phosphates and upon extra- and intracellular lactate, pyruvate and bicarbonate concentrations in the rat brain. *Acta Physiol Scand* 1970; 80: 235–248.
 79. Sonnay S, Duarte JMN, Just N, et al. Energy metabolism in the rat cortex under thiopental anaesthesia measured *In Vivo* by ¹³C MRS. *J Neurosci Res* 2017; 95: 2297–2306.
 80. Swain JA, McDonald TJ, Balaban RS, et al. Metabolism of the heart and brain during hypothermic cardiopulmonary bypass. *Ann Thorac Surg* 1991; 51: 105–109.
 81. Friedman SD, Jensen JE, Frederick BB, et al. Brain changes to hypocapnia using rapidly interleaved phosphorus-proton magnetic resonance spectroscopy at 4T. *J Cereb Blood Flow Metab* 2007; 27: 646–653.
 82. Schneider GH, Sarrafzadeh AS, Kiening KL, et al. Influence of hyperventilation on brain tissue-PO₂, PCO₂, and pH in patients with intracranial hypertension. *Acta Neurochir Suppl* 1998; 71: 62–65.

83. Garnett MR, Blamire AM, Corkill RG, et al. Early proton magnetic resonance spectroscopy in normal-appearing brain correlates with outcome in patients following traumatic brain injury. *Brain* 2000; 123(Pt 1): 2046–2054.
84. Uzan M, Albayram S, Dashti SGR, et al. Thalamic proton magnetic resonance spectroscopy in vegetative state induced by traumatic brain injury. *J Neurol Neurosurg Psychiatry* 2003; 74: 33–38.
85. Ricci R, Barbarella G, Musi P, et al. Localised proton MR spectroscopy of brain metabolism changes in vegetative patients. *Neuroradiology* 1997; 39: 313–319.
86. Friedman SD, Brooks WM, Jung RE, et al. Proton MR spectroscopic findings correspond to neuropsychological function in traumatic brain injury. *AJNR Am J Neuroradiol* 1998; 19: 1879–1885.
87. Lee S-Y, Kim SS, Kim C-H, et al. Prediction of outcome after traumatic brain injury using clinical and neuroimaging variables. *J Clin Neurol* 2012; 8: 224–229.
88. Coles JP. Imaging after brain injury. *Br J Anaesth* 2007; 99: 49–60.
89. Marino S, Ciurleo R, Bramanti P, et al. 1H-MR spectroscopy in traumatic brain injury. *Neurocrit Care* 2011; 14: 127–133.
90. Signoretti S, Marmarou A, Aygok GA, et al. Assessment of mitochondrial impairment in traumatic brain injury using high-resolution proton magnetic resonance spectroscopy. *J Neurosurg* 2008; 108: 42–52.
91. Shutter L, Tong KA, Lee A, et al. Prognostic role of proton magnetic resonance spectroscopy in acute traumatic brain injury. *J Head Trauma Rehabil* 2006; 21: 334–349.
92. Carpentier A, Galanaud D, Puybasset L, et al. Early morphologic and spectroscopic magnetic resonance in severe traumatic brain injuries can detect “invisible brain stem damage” and predict “vegetative states”. *J Neurotrauma* 2006; 23: 674–685.
93. Steyerberg EW, Mushkudiani N, Perel P, et al. Predicting outcome after traumatic brain injury: development and international validation of prognostic scores based on admission characteristics. *PLoS Med* 2008; 5: e165; discussion e165.